CHIN. PHYS. LETT. Vol. 33, No. 7 (2016) 078101

Growth of Ag on Pb Island with Si(111) Substrate *

Xiao-Peng Hu(胡小鹏)[1,2,3], Rui Zhu(朱瑞)[1,3], Jun Xu(徐军)[1,3], Shuai-Hua Ji(季帅华)[2,3**], Xi Chen(陈曦)[2,3], Qi-Kun Xue(薛其坤)[2,3], Da-Peng Yu(俞大鹏)[1,3]

[1]*State Key Laboratory for Mesoscopic Physics and Electron Microscopy Laboratory, School of Physics, Peking University, Beijing 100871*

[2]*State Key Laboratory of Low-Dimensional Quantum Physics, Department of Physics, Tsinghua University, Beijing 100084*

[3]*Collaborative Innovation Center of Quantum Matter, Beijing 100084*

(Received 14 April 2016)

We study the growth of Ag on Pb island surface with low temperature scanning tunnelling microscopy. Two growth modes, the subsurface island mode and the surface alloy mode, are observed on the substrate at room temperature and at 100 K, respectively. In the surface alloy mode, the perfect alloy $AgPb_2$ is formed on the Pb island surface after annealing. The two growth modes at different substrate temperatures are attributed to the existence of an exchange barrier of Ag atoms on the Pb island surface. The modulation of the exchange barrier by the quantum well states is also observed on the Pb island.

PACS: 81.15.Hi, 07.79.Fc, 68.35.Md, 81.07.St DOI: 10.1088/0256-307X/33/7/078101

Epitaxial growth of metal elements on metal substrates has attracted great attention during the past several decades due to the fundamental interests and the potential applications. In recent years, a new growth mode has been discovered when metals with high surface energy are deposited on the low energy metal surfaces.[1–4] In this mode, a single layer of substrate metal atoms floats on the top of the deposited metal, which is different from the three well-known basic growth modes (Frank–van der Merwe, Stranski–Krastanov, and Volmer–Weber). Furthermore, two immiscible metals in the bulk have been found to form a stable surface alloy.[5–11] The electronic hybridization of two different species offers the possibility to design new materials on the surface with unique chemical or physical properties, for example, the giant spin-orbit splitting observed in the surface alloy Bi/Ag(111).[12] Here we report the growth of Ag on Pb island surface, which are immiscible in bulk. In previous reports, only growth of Ag on bulk Pb(111) surface[13] or Pb on Ag(111)[14,15] surface have been studied. The influence of substrate temperature and quantum well state on the growth have not been systematically studied. By varying the substrate temperature, two distinguished growth modes have been observed as Ag atoms are deposited on Pb island surface. In addition, we observe the formation of surface alloy consisting of Ag and Pb.

The experiment was conducted on a Unisoku UHV He3 scanning tunnelling microscope (STM) with a base pressure of 1×10^{-10} Torr. The preparation of Pb islands on the clean Si(111)-7 × 7 reconstruction surface is similar to those in the literature.[16–19] Ag (99.9999%) was evaporated at a rate of 0.37 monolayer (ML)/min, which was estimated by the STM image of Ag islands grown on a silicon substrate. During the evaporation of Pb and Ag, the vacuum pressure was kept at 1×10^{-9} Torr. In the experiments, the STM imaging and scanning tunnelling spectroscopy (STS) measurement were conducted at the liquid helium temperature. The differential tunnelling conductance dI/dV was measured by the lock-in technique with a modulation voltage of 0.01 V at 1.991 kHz when the feedback loop was turned off.

We first kept the Pb island at room temperature during Ag deposition. Islands with Moiré pattern appeared on the terraces of Pb surface after deposition (Figs. 1(a) and 1(b)). This growth behavior of Ag on Pb(111) surface is exactly the same as the subsurface growth mode of Cu on Pb(111),[4] as a result of minimization of the surface energy. The Moiré pattern comes from the overlap between the subsurface Ag island and the single layer of Pb floated on the top. According to this model, the islands A and B in Fig. 1(b) should have a single Ag layer thickness difference. The profile line located on the black line in Fig. 1(b) is shown in Fig. 1(c). The height difference between islands A and B is about 0.22 nm and it is quite close to the single Ag layer thickness 0.236 nm. The period of the Moiré pattern, 1.68±0.06 nm, is consistent with 1.66 nm which is modelled by overlapping the lattice of Ag(111) and Pb(111) surface with the same orientation. By the best fit, the height difference between island B and surrounded Pb terrace gives the thickness of the underneath Ag island, 3 ML. Figure 1(e) indicates the model of the above cross section. Another strong evidence of the this model is that the lattice constant and orientation on the Moiré pattern area is the same as the surrounded Pb terrace, as shown in Fig. 1(d) with the atomic resolution.

The growth behavior of Ag on Pb(111) at low temperature is completely different from room tempera-

*Supported by the National Natural Science Foundation of China, and the Ministry of Science and Technology of China.

**Corresponding author. Email: shji@mail.tsinghua.edu.cn

© 2016 Chinese Physical Society and IOP Publishing Ltd

ture, at low temperature the thermal driving subsurface growth mode has been hindered. The 0.56 ML Ag was deposited on the Pb(111) island surface kept at around 106 K. After the deposition, the sample was immediately transferred to the low temperature STM without any annealing. Figure 2(a) shows the morphology of the Pb(111) surface after the Ag deposition. At the first glance, the islands have the fractal shape. On closer inspection, there are two features of the islands. One is the relatively flat fractal island with the height of 0.232 nm as indicated by the arrows in Fig. 2(a). The other is the nanopucks which is randomly decorated on the first one. These nanopucks, we believe, are the Ag clusters as reported before.[20]

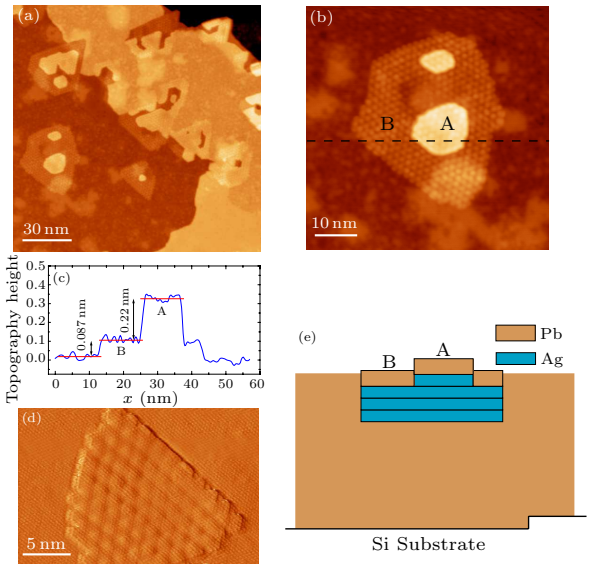

Fig. 1. (a) The morphology of Pb island surface after deposition of Ag (150×150 nm, $V = 0.5$ V and $I = 0.1$ nA). (b) STM image on the top of subsurface growth mode island (57×57 nm, $V = 0.5$ V and $I = 0.1$ nA). (c) The cross section indicated by the dashed line in (b). (d) The atomic resolution on the Moiré pattern ($V = -0.5$ V and $I = 0.1$ nA). (e) The model of the subsurface growth mode in (b).

The average of their height was estimated to be 0.39 nm. After transferring the sample to room temperature environment and annealing for 20 min, the flat island with the single layer thickness of about 0.18 nm has been formed on the Pb(111) surface and the Ag cluster almost completely disappeared (Fig. 2(b)). As we deposited additional 0.56 ML Ag at the same temperature with the post annealing 20 min as before, the island on the Pb(111) surface will continue to grow. The average size of the island has been increased as indicated in Fig. 2(c). On the other hand, the long range hexagonal Moiré patterns have been clearly resolved on the top of the island. These patterns are due to the lattice overlapping between the substrate and the island (Fig. 2(d)). Under the atomic resolution tip condition, both lattices of the island and the substrate have been revealed in Fig. 2(e). With the information of the lattice orientation (the white dashed line in Fig. 2(e)), the $(\sqrt{3}\times\sqrt{3})$R30°Ag/Pb(111) lattice has been determined on the top of the island. The similar structure has been reported on the Pb/Ag(111) system.[14,15] The $(\sqrt{3}\times\sqrt{3})$R30°Pb/Ag(111) was formed with one Pb atom surrounded by six Ag atoms in the lattice. In our case, we believe that $AgPb_2$ surface alloy has been formed with one Ag atom surrounded by six Pb atoms due to the minimization of the lattice mismatch with the Pb(111) substrate. The dips on top of the islands represent the Ag atoms' positions and the protrusions are Pb atoms due to the small size of Ag atoms compared with the Pb atoms. The protrusions and the dips in the image are inverse compared with the STM image in the previous report.[14] The top view and side view of the $AgPb_2$ surface alloy model has been shown in Figs. 2(f) and 2(g). With the hexagonal Moiré pattern's average lattice constant in Fig. 3(b), about 7.4 nm, the average distance between two atoms in the surface alloy is about $0.95a_{\rm Pb}$, where $a_{\rm Pb}$ is the lattice constant of Pb(111) surface.

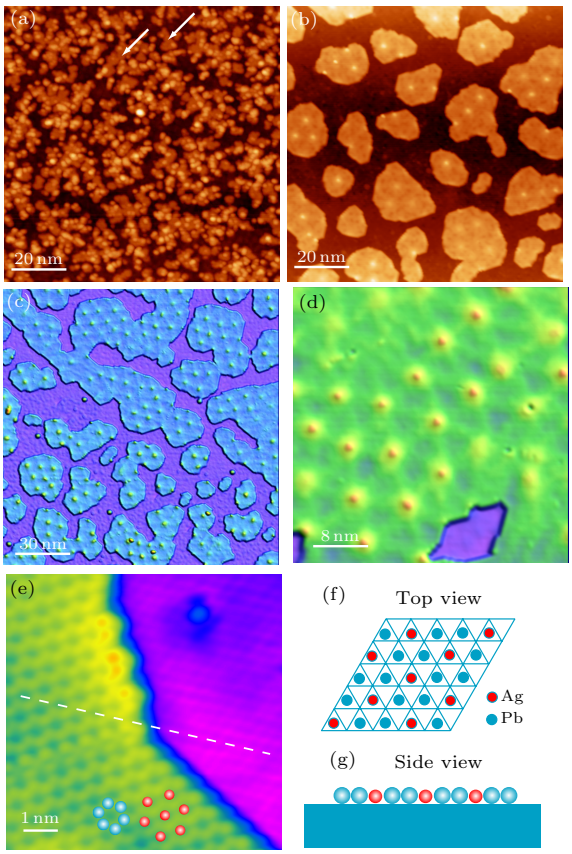

Fig. 2. (a) The morphology after deposition of Ag on Pb island at 106 K (100×100 nm, $V = 1$ V and $I = 0.1$ nA). (b) The surface alloy island after annealing (100×100 nm, $V = 0.6$ V and $I = 0.1$ nA). (c) The larger surface alloy island after additional deposition and annealing (150×150 nm, $V = 1.4$ V and $I = 0.1$ nA). (d) The hexagonal Moiré pattern on the surface alloy (40×40 nm, $V = 0.1$ V and $I = 0.1$ nA). (e) The atomic resolution on the surface alloy and the substrate (8×8 nm, $V = 10$ mV and $I = 0.1$ nA). Here (f) and (g) are the top view and the side view of the surface alloy model.

These two different growth modes are controlled by

the thermal energy. At room temperature or above, the mobility of both atoms are high and the atomic exchange process is triggered by the thermal energy. The morphology after the deposition is the energy favored stable state. This thermal equilibrium state has the lowest total free energy at the specified configuration. As the surface energy of Pb(111) is smaller than the Ag, the 3D island growth mode would be expected. Nevertheless, due to the low surface energy of the Pb and the interface, the total free energy of the subsurface growth mode, e.g., $\gamma_i+\gamma_i'+\gamma_{\rm Pb}$, is smaller than the free energy of the 3D island, e.g., $\gamma_i+\gamma_{\rm Ag}$. Thus this is the reason why we see the embedded Ag island during the growth. However, at the low temperature, the exchange barrier of the Ag atoms with Pb atoms on the surface has hindered the exchange process. The Ag nucleation happened on the Pb surface and the cluster on the Pb surface. During the deposition, there are also the mobile Pb adatom on the surface and the $AgPb_2$ surface alloy has been formed. Since the density of the Pb adatom is smaller than the density of the Ag adatom during the deposition, both the Ag cluster and the $AgPb_2$ surface alloy have been observed. The ultra thin Pb film on a Si(111) substrate exhibits the magic thickness,[21] which shows that the confined electrons in the thin film influence the growth of the Pb film. Not only the growth but also these quantum well states modulate the physical and chemical property of the thin film, such as superconductivity, work function, chemical reactivity, the Kondo resonance.[16–19,22] We also find this quantum effect on the Ag growth on the Pb film. We deposit 1.28 ML Ag on the Pb/Si(111) and post anneal the sample at room temperature environment for 30 min. The island surface was almost fully covered with $AgPb_2$ surface alloy and small vacancy islands as shown in Fig. 3(a). The dI/dV measured in the vacancy area can be used to identify the thickness of the Pb film underneath the surface alloy by the unique quantum well state features of each Pb film thickness. The dI/dV curve shown in Fig. 3(c) indicates that the thicknesses of the Pb films are 12 ML, 13 ML and 14 ML from bottom to top in Fig. 3(a). On the 13 ML, vacancy island area is larger compared with the 12 ML and 14 ML. Some thicker islands appear at the edge or inside of the $AgPb_2$ surface alloy interconnected islands. From the thickness and the Moiré patterns (Fig. 3(b)), they can be identified as the subsurface growth islands as we observed at room temperature. From the previous reports, 12 ML and 14 ML are stable and have lower surface energies compared with the 13 ML. It can be easily expected that Pb atoms on the 13 ML has lower exchange barrier with Ag atoms compared with 12 ML and 14 ML. During the annealing process, the thermal energy has overcome the exchange barrier on 13 ML and the subsurface Ag island with a single Pb layer on the top has been formed. The higher exchange barrier on 12 ML and 14 ML hinders this process and no subsurface Ag island has been observed. This experiment directly demonstrates that the quantum well states in the Pb film modulate the atomic exchange barrier of Ag atoms on Pb surface. The dI/dV curve is also conducted on the surface alloy surface on the 12 ML as shown in Fig. 3(c) (red curve). The single layer surface alloy acts like a single layer of Pb atoms. The positions of peaks in dI/dV on the surface alloy on the 12 ML substrate are almost the same as the 13 ML. The broadening of the peaks on surface alloy may be due to the increase of the surface scattering on the surface alloy.

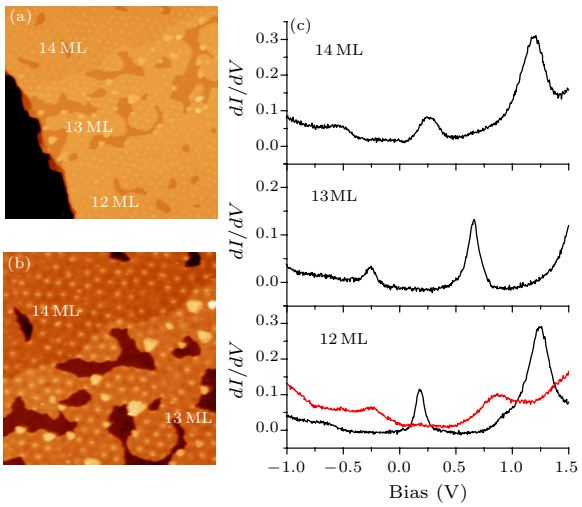

Fig. 3. (a) STM image of surface alloy on 12 ML, 13 ML and 14 ML after annealing (200 × 200 nm, $V = 1.0$ V and $I = 0.06$ nA). (b) STM image of the surface alloy and the small subsurface Ag island on 13 ML (120 × 120 nm, $V = 1.0$ V and $I = 0.06$ nA). (c) The black curves show dI/dV on the vacancy on different layers. The red curve shows dI/dV on the surface alloy on 12 ML.

In summary, we have systematically studied the Ag growth on the Pb/Si(111) at different temperatures. It is revealed that the subsurface growth mode appears at room temperature and the nano-clusters and surface alloy form as the substrate is kept at 100 K. With the post annealing, the perfect $AgPb_2$ surface alloy has been obtained on the Pb(111) surface. At room temperature, the embedded Ag islands with a single layer of Pb floated on the top has the lower total free energy. However, at the low temperature of 100 K, we expect that the thermal energy is lower than the exchange barrier of Ag atoms on the Pb(111) surface and the atomic exchange process is hindered. As a sequence, the Ag clusters and the $AgPb_2$ surface alloy are formed on the Pb(111) surface. We also observe that the quantum well states in the Pb film modulate this exchange barrier. The conclusion of this work may extend to the other systems in which the high surface energy metal is deposited on the lower surface energy metals. We also find a way to prepare the perfect surface alloy by low temperature deposition and post annealing, and this method can also be adopted in other systems.

The STM topographic images were processed us-

ing WSxM (www.nanotec.es).

References

[1] Taylor T N and Campbell C T 1993 *Surf. Sci.* **280** 277
[2] Bader S D and Moog E R 1987 *J. Appl. Phys.* **61** 3729
[3] Schmitz P J, Leung W Y, Graham G W and Thiel P A 1989 *Phys. Rev.* B **40** 11477
[4] Nagl C, Platzgummer E, Schmid M, Varga P, Speller S and Heiland W 1995 *Phys. Rev. Lett.* **75** 2976
[5] Röder H, Schuster R, Brune H and Kern K 1993 *Phys. Rev. Lett.* **71** 2086
[6] Oppo S, Fiorentini V and Phys M 1993 *Phys. Rev. Lett.* **71** 2437
[7] Bardi U 1994 *Rep. Prog. Phys.* **57** 939
[8] Tersoff J 1995 *Phys. Rev. Lett.* **74** 434
[9] Stevens J L and Hwang R Q 1995 *Phys. Rev. Lett.* **74** 2078
[10] Quinn P D, Bittencourt C and Woodruff D P 2002 *Phys. Rev.* B **65** 233404
[11] Shu X K, Jiang P and Che J G 2003 *Surf. Sci.* **545** 199
[12] Christian R A, Henk J, Ernst A, Moreschini L, Falub M C, Pacile D, Bruno P, Kern K and Grioni M 2007 *Phys. Rev. Lett.* **98** 186807
[13] Chen C H and Sansalone F J 1985 *Surf. Sci.* **163** L688
[14] Dalmas J, Oughaddou H, Léandri C, Gay J M, Lay G L, Tréglia G, Aufray B, Bunk O and Johnson R L 2005 *Phys. Rev.* B **72** 155424
[15] Pacilé D, Ast C R, Papagno M, Silva C D, Moreschini L, Falub M, Seitsonen A P and Grioni M 2006 *Phys. Rev.* B **73** 245429
[16] Ma X C, Jiang P, Qi Y, Jia J F, Yang Y, Duan W H, Li W X, Bao X H, Zhang S B and Xue Q K 2007 *Proc. Natl. Acad. Sci. USA* **104** 9204
[17] Qi Y, Ma X C, Jiang P, Ji S H, Fu Y S, Jia J F, Xue Q K and Zhang S B 2007 *Appl. Phys. Lett.* **90** 013109
[18] Ma L Y, Tang L, Guan Z L, He K, An K, Ma X C, Jia J F, Xue Q K, Han Y, Huang S and Liu F 2006 *Phys. Rev. Lett.* **97** 266102
[19] Fu Y S, Ji S H, Chen X, Ma X C, Wu R, Wang C C, Duan W H, Qiu X H, Sun B, Zhang P, Jia J F and Xue Q K 2007 *Phys. Rev. Lett.* **99** 256601
[20] Lin H Y, Chiu Y P, Huang L W, Chen Y W, Fu T Y, Chang C S and Tsong T T 2005 *Phys. Rev. Lett.* **94** 136101
[21] Su W B, Chang S H, Jian W B, Chang C S, Chen L J and Tsong T T 2001 *Phys. Rev. Lett.* **86** 5116
[22] Guo Y, Zhang Y F, Bao X Y, Han T Z, Tang Z, Zhang L X, Zhu W G, Wang E G, Niu Q, Qiu Z Q, Jia J F, Zhao Z X and Xue Q K 2004 *Science* **306** 1915